PROCEEDINGS OF SCIENCE

Searches for Point-Like and Extended Sources of Cosmic Neutrinos with the Complete ANTARES Dataset

Sergio Alves Garre,[a] **Giulia Illuminati,**[b] **Francisco Salesa Greus**[a,*] **and Agustín Sánchez Losa**[a] **on behalf of the ANTARES Collaboration**

[a] *Instituto de Física Corpuscular (Universtitat de València - CSIC),*
Carrer del Catedràtic José Beltrán 2, 46980, Paterna, Valencia, Spain
[b] *INFN - Sezione di Bologna,*
Viale Berti-Pichat 6/2, 40127 Bologna, Italy

E-mail: sagreus@ific.uv.es

The ANTARES neutrino telescope was a 0.01 km^3 volume detector located at the bottom of the Mediterranean Sea. It operated from 2007 until early 2022, and over its 15-year span it accumulated valuable neutrino data. The primary goal of ANTARES was to detect neutrinos originated at astrophysical sources. Thanks to the optical properties of the sea water, ANTARES was able to reconstruct neutrino events with an angular resolution better than 0.4 degrees at the highest energies, with a privileged view of the Galactic sky thanks to its location.

Throughout its operation, the ANTARES Collaboration regularly updated its findings on astrophysical neutrino emissions. Now, with the detector decommissioned, the final analysis using the complete dataset and most refined selection is presented in this contribution. The study looks for potential Galactic and extragalactic sources of high energy neutrinos, with point-like and extended assumptions on the spatial emission profile. It also includes a search for neutrino clustering across the entire sky visible to the ANTARES telescope, as well as a dedicated survey of the Galactic Plane.

39th International Cosmic Ray Conference (ICRC2025)
15–24 July 2025
Geneva, Switzerland

ICRC 2025
The Astroparticle Physics Conference
Geneva July 15-24, 2025

*Speaker

PoS(ICRC2025)1191

1. Introduction

More than a century after their discovery, our understanding of the origin of high-energy cosmic rays remains limited. One way to learn about the sources and the acceleration mechanisms involved is through neutrino astronomy, i.e., observing the Universe using neutrinos as cosmic probes. Neutrinos have the advantage that they are neither deflected nor absorbed on their way to Earth, so they can point back to their sources and come from remote regions of the Universe. Moreover, neutrinos are expected to originate in hadronic interaction scenarios, where cosmic and gamma rays should also be produced. Therefore, the detection of a cosmic neutrino source would indicate that high-energy cosmic rays are being accelerated at the source. Doing astronomy with neutrinos is one of the main goals of neutrino telescopes. However, this is challenging due to the low statistics these detectors collect, as a consequence of the small interaction cross-section of neutrinos. Neutrino astronomy requires instrumenting large detection volumes in optically transparent media, such as seawater, in order to detect the Cherenkov light produced by secondary particles resulting from cosmic neutrinos interacting with matter.

ANTARES was a first-generation neutrino telescope installed at the bottom of the Mediterranean Sea, operating from 2007 to 2022. In ANTARES analyses, we typically distinguish between two types of events, tracks and showers, based on the Cherenkov light signatures produced in water. Track events are usually produced by long-lived relativistic muons resulting from charged current interactions of muon neutrinos (ν_μ), which leave a characteristic elongated light pattern. Shower events, on the other hand, are primarily produced by charged current interactions of electron neutrinos (ν_e) and tau neutrinos (ν_τ), as well as by neutral current interactions of all neutrino flavors. The final ANTARES data set used in the analyses presented here includes 11029 track events and 200 shower events.

2. Search methodology

The small amount of signal expected from cosmic neutrino sources has to be tested against the dominant background, which typically comes from two main sources. First, from muons created after the interaction of cosmic rays with the atmosphere. This flux of atmospheric muons is several orders of magnitude higher compared to the expected signal flux. Fortunately, this flux can be severely suppressed by selecting only upward reconstructed events for our analysis. In this case, the Earth acts as a shield and, therefore, the only surviving muons are those produced after a neutrino interaction nearby the detector. Even after this selection, some misreconstructed events can still mimic a genuine neutrino-induced muon. To address this, a stricter event selection based on the quality of the event reconstruction can reduce the atmospheric muons to a subdominant contribution. There is also an irreducible contribution coming from neutrinos produced in the atmosphere after cosmic ray interactions. Here, we have two ways to tell apart signal from background. First we expect the atmospheric neutrino background to be isotropically distributed, while cosmic neutrino signal should accumulate around the source location in the sky. In addition, we expect atmospheric neutrinos to present a softer spectrum than cosmic neutrinos, e.g. [1]. Therefore, we can use the reconstructed energy of the events as a discriminating parameter.

In order to evaluate the presence of signal in our data we use a likelihood statistical method. First, we assume that the individual probability for each event is:

$$f(\vec{x}_i \mid \vec{\theta}) = \frac{n_S}{N} S(\vec{x}_i) + \left(1 - \frac{n_S}{N}\right) B(\vec{x}_i), \tag{1}$$

where $S(\vec{x}_i)$ and $B(\vec{x}_i)$ describe the signal and background probability density functions. In that case, the likelihood of observing a set of N independent observations $\vec{x}_i$ is given by the product of the probabilities, which typically is written in its logarithm form for simplicity:

$$\log \mathcal{L}(n_S) = \sum_{i=1}^{N} \log(f(\vec{x}_i \mid \vec{\theta})) = \sum_{i=1}^{N} \log\left(\frac{n_S}{N} S(\vec{x}_i) + \left(1 - \frac{n_S}{N}\right) B(\vec{x}_i)\right). \tag{2}$$

Maximizing this likelihood allows us to find the number of signal events (n_S) that makes the data most likely under the assumed model. To evaluate how well the signal-plus-background hypothesis (obtained from the likelihood maximization) describes the data compared to a background-only scenario, we perform a Likelihood Ratio Test. We define our Test Statistic (TS) as:

$$\mathrm{TS} = -2 \log\left(\frac{\mathcal{L}(n_S = 0)}{\mathcal{L}(\hat{n}_S)}\right) = 2(\log \mathcal{L}(\hat{n}_S) - \log \mathcal{L}(n_S = 0)). \tag{3}$$

Finally, we want to assess how significant our observation is. For that, we simulate pseudo-experiments that contain only background events and compute the TS for each simulation. We then generate TS distribution for the background-only hypothesis so we can see how unusual our observed TS is. By comparing the observed TS to the background only hypothesis we obtain the p-value that we can later convert to a Gaussian Z-score. In our case, using a one-sided Gaussian convention[1].

For our analyses, we consider a spectral signal hypothesis modeled as a simple power law, $\Phi = \Phi_0 E^{-\gamma}$, with a spectral index $\gamma = 2$ and 2.5, and a spatial morphology that can be either a point source or an extended two-dimensional Gaussian with width σ_e, depending on the analysis.

3. Results

With the methodology explained in the previous section three searches have been performed.

3.1 All-sky

In the first search the goal is to identify cosmic neutrino sources without any previous assumption about their location. For that we use a grid pixelization based on HealPix [2] using a Nside = 512, i.e., approximately 0.11° x 0.11° pixel size, which is smaller than the typical ANTARES angular resolution[2] of 0.5°.

For every pixel in the grid we compute the p-value assuming that the signal neutrino flux has a spectral index of $\gamma = 2$ and the emission comes from a point source.

[1] A one-sided significance assumes the signal can only manifest as an excess over the background, while a two-sided allows for deviations in both directions (excess or deficit). In neutrino astronomy, a one-sided convention is typically used, since we search for an excess of events above the expected background.

[2] The median angular resolution is defined as the radius around the true neutrino direction in which 50% of events are reconstructed. The angular resolution depends on the selection cuts applied.

Considering the location of ANTARES (42°48' N) and that we restrict our analysis to up-going reconstructed events, the detector visibility decreases at high-declination angles. For that reason, our searches are restricted to declination angles lower than 40°. The results of the analysis can be visualized in Fig. 1.

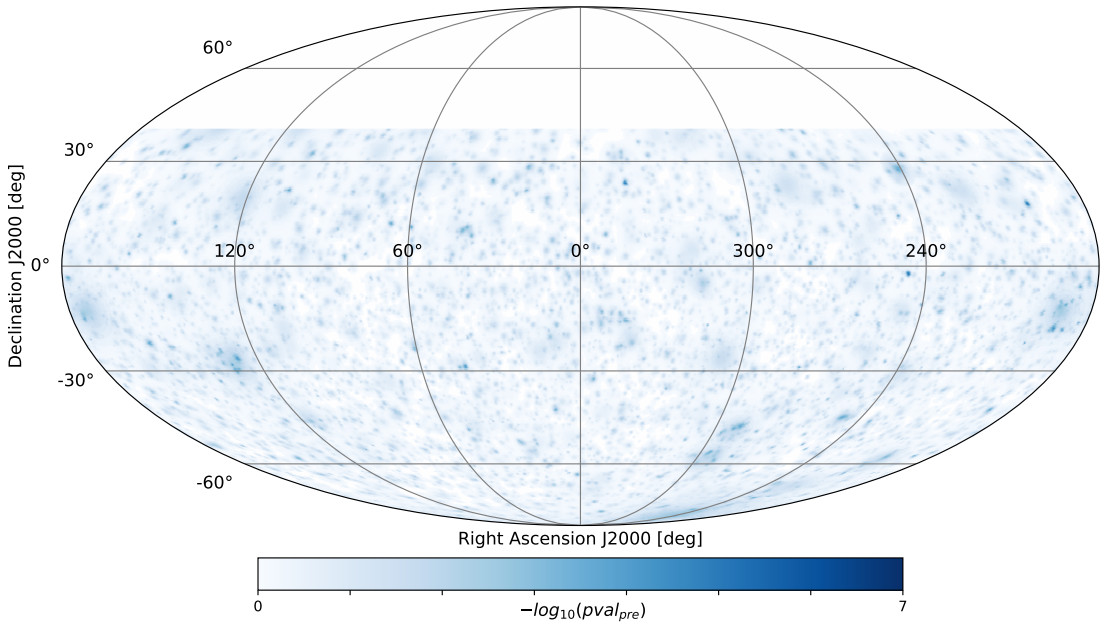

Figure 1: Skymap in equatorial coordinates in Mollweide projection, showing the -log(p-value) for each pixel. The pixelization is based on HealPix with Nside = 512, and the values are represented using a blue color scale, where darker shades indicate higher significance. The p-values are calculated for a point source hypothesis with a spectral index of $\gamma = 2$.

The most significant pixel was found at the location (R.A., dec) = (200.5°, 17.7°) with a fitted signal of 2.23 events. This translates to a p-value of 3.23×10^{-6} which is equivalent to 4.5σ in the one-sided convention. Given that the grid used for the analysis includes more than 2 million pixels, we need to correct our p-value to account for the look elsewhere effect. The corrected p-value is 0.38 which is compatible with the excess being produced by a background fluctuation. In any case, we have searched for potential astrophysical counterparts to the best pixel (see Fig.2 left). The closest source was about one degree away which, given the angular resolution of ANTARES, means that there is no compelling evidence for an association.

3.2 Targeted search

One way to reduce the intrinsic large trial factor penalization of the all-sky search is to elaborate a list of candidates sources with great potential for emitting high-energy cosmic neutrinos. The list used is a compilation of Galactic and extragalactic sources including for instance, high-energy gamma-ray sources from TeVCat [4], blazars, starburst galaxies, IceCube interesting observations, among others.

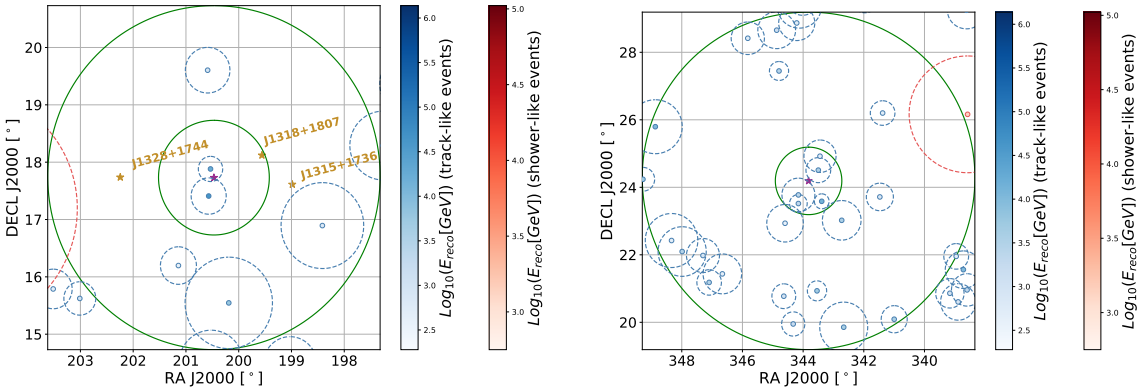

(a) (b)

Figure 2: Zoom in of the most interesting spots for the all-sky search (left) and the targeted search (right). The green circles are used for reference and have 1° and 5° radius, centered at the best pixel (left) or source location (right). The events, tracks (blue) or shower-like (red) are represented as circles filled with a color which intensity represents the energy estimated. The dashed circles represent the angular error of the event.

The total number of sources tested are 169 out of which 14 are extended. For this search we tested two spectral indices, 2 and 2.5, and a 2D-Gaussian morphology based on the source size in gamma rays. The results with the different spectral indices are comparable so in these proceedings we report only the results for the index $\gamma = 2$ case in Table 1. The table shows only the sources that has some fitted signal, with the most significant ones (above 2σ) highlighted. The complete list and the other spectral hypothesis tested can be found in [3].

Even if none of the sources in the catalog are significant after trial correction, it is worth to mention some interesting cases like the radio blazars MG3 J225517+2409 (see Fig.2 right) and 3C403 with 3.5 and 3.3 σ pre-trial significance, respectively.

In the list of seven sources above above 2σ pre-trial significance we found the well-known TXS 05056+056 [5] the Galactic Center, and Vela X. It is worth mentioning that the significance of Vela X increased from 1.3 to 1.92 σ when the source extension is taken into account, rather than assuming it is point-like as in the previous analysis [6].

It is important to note that none of these observations provides statistically significant evidence to claim a detection. However, given the limited detection volume of ANTARES, such mild excesses are consistent with what one might expect from a genuine neutrino source. Fortunately, the next-generation neutrino telescope in the Mediterranean, KM3NeT, is currently under construction, and a partial configuration is already taking data. The KM3NeT sensitivity is expected to be an order of magnitude greater than that of ANTARES, sufficient to confirm or rule out the excesses observed in the ANTARES data.

Since no significant detections were found, upper limits were derived (see Fig. 3).

3.3 Galactic Plane survey

In addition to the previous searches, a dedicated search focused on the Galactic Plane has also been done. Gamma-ray observations by ground-based detector have shown that extended emission is quite common in the Galactic Plane. Because of that, in order to be more sensitive

Table 1: Source candidates with their equatorial celestial coordinates, source extension, fitted number of signal events, pre-trial p-value, and 90% C.L. upper limits on the flux normalization for a $E^{-2.0}$ spectrum (in units of 10^{-8} GeV cm^{-2} s^{-1}). The table reports only the sources with fitted signal out of 169 in the list explored. Source with pre-trial significance above 2σ are highlighted.

Name	δ [°]	α [°]	σ_e [°]	$\hat{n}_{\rm sig}$	p-value	$\phi_0^{90\%\text{C.L.}}$
IC hotspot South	-56.5	350.2	–	0.3	0.16	0.64
PKS 2005-489	-48.82	302.37	–	0.6	0.16	0.55
HESS J1641-463	-46.31	250.26	–	1.26	0.11	0.68
Westerlund 1	-45.85	251.76	0.61	1.04	0.15	0.68
Vela X	**-45.60**	**128.75**	**0.58**	**2.76**	**0.027**	**0.97**
Centaurus A	-43.02	201.36	–	0.96	0.064	0.78
PKS 1454-354	-35.67	224.36	–	0.28	0.17	0.73
HESS J1741-302	-30.38	265.32	–	0.8	0.12	0.80
Galactic Centre	**-29.01**	**266.43**	–	**2.06**	**0.017**	**1.18**
J0609-1542	**-15.71**	**92.42**	–	**1.22**	**0.0073**	**1.41**
QSO 1730-130	-13.10	263.30	–	1.33	0.077	1.00
PKS 0727-11	-11.70	112.58	–	1.37	0.041	1.13
HESS J1828-099	-9.99	277.24	–	0.83	0.076	1.05
J0607-0834	-8.58	-92	–	0.59	0.152	0.97
QSO 2022-077	-7.60	306.40	–	0.45	0.13	0.92
RS Ophiuchi	-6.71	267.55	–	1.07	0.031	1.22
J0006-0623	-6.39	1.56	–	1.50	0.033	1.20
3C279	-5.79	194.05	–	1.42	0.065	1.07
PKS 1741-038	-3.83	266	–	1.65	0.038	1.20
J2136+0041	0.70	324.16	–	0.16	0.176	0.91
3C403	**2.51**	**298.07**	–	**2.47**	**0.00048**	**2.02**
TXS 0506+056	**5.7**	**77.35**	–	**2.23**	**0.0075**	**1.6**
HESS J0632+057	5.81	98.24	–	1.4	0.033	1.31
W 49B	9.09	287.78	–	0.96	0.039	1.27
J0242+1101	**11.02**	**40.6**	–	**3.67**	**0.0074**	**1.58**
J1230+1223	12.39	187.71	–	0.45	0.173	1.01
J0750+1231	12.52	117.72	–	1.62	0.084	1.14
RGB J2243+203	20.5	340.98	–	0.72	0.109	1.15
MG3 J225517+2409	**24.19**	**343.82**	–	**3.97**	**0.00024**	**2.28**
3HWC J1950+242	24.26	297.69	–	0.52	0.11	1.13
PKS 1441+25	25.03	220.99	–	0.61	0.12	1.12
J0927+3902	39.04	141.76	–	0.13	0.162	1.22

than the traditional point-like source search done for the all-sky search, we test four different source extensions (σ_e): 0.5°, 1°, 1.5°, and 2°. In this search, no source position is assumed and all the pixels in the inner Galaxy, defined by $|b| < 5$, are tested.

The best spot for the Galactic Plane survey is found at the location with Galactic coordinates (l,b) = (-20.73°, 2.59°), for all 4 cases, the one with 0.5° being the most significant one with a p-value of 2.96×10^{-4} which goes to 0.6 after trial correction. Again, this search is compatible with background fluctuations. Fig. 4 shows the result of the search for the case of the 1° extension.

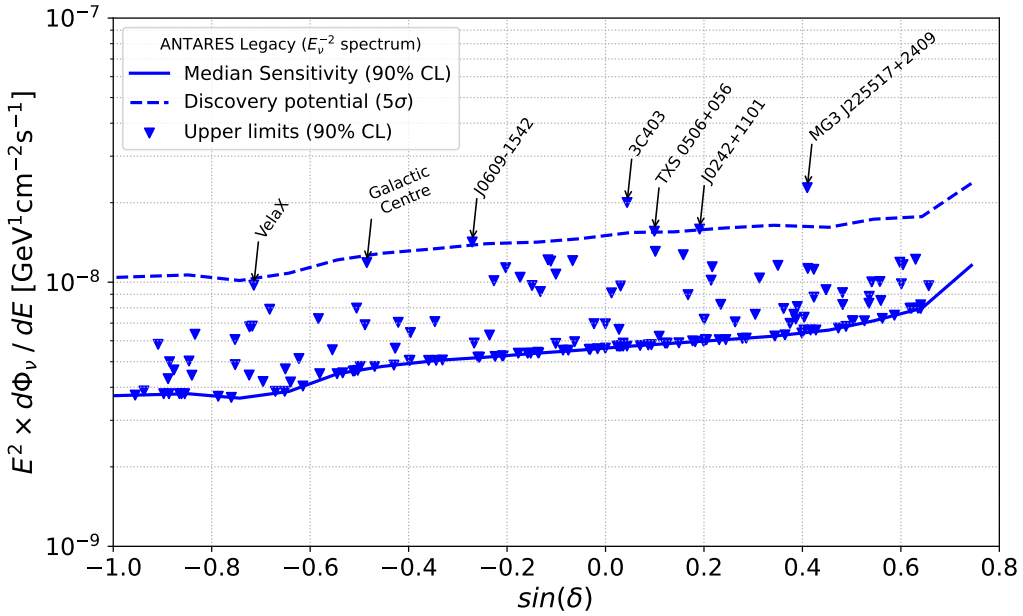

Figure 3: Flux upper limits for the 169 sources targeted (blue triangles). The lines represent the median sensitivity at 90% C.L. (solid) and the 5σ discovery flux (dashed). The seven sources exceeding a 2σ pre-trial significance are labeled.

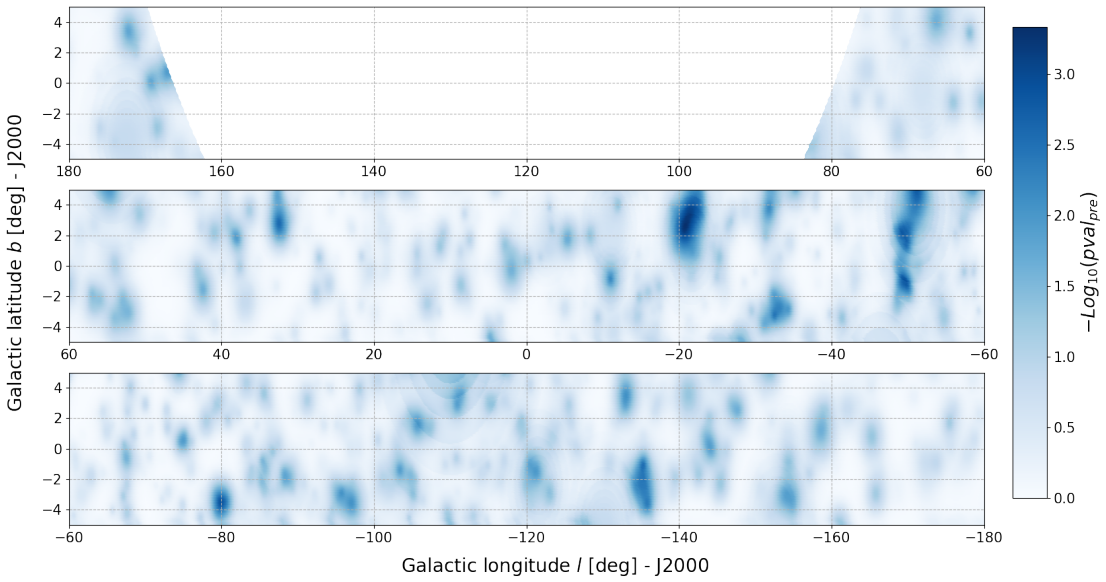

Figure 4: Inner Galactic plane region, in Galactic coordinates. The -log(p-value) is calculated for assuming a source extension of 1° and a spectral index of $\gamma = 2$.

4. Conclusions

A search for cosmic neutrino sources using data from the complete ANTARES dataset has been performed using a maximum likelihood method to evaluate the significance with respect to the background fluctuations.

We presented the results for the three different types of searches performed. None of the searches yielded significant source detection. However, several interesting excesses have been identified. These potential candidates will be tested with the next generation KM3NeT detector [7].

Acknowledgements

The speaker acknowledges the support of the Consejo Superior de Investigaciones Científicas (CSIC) through the incorporation grant for Research Scientists (OEP 2022), reference 2025ICT054.

References

[1] R. Abbasi *et al.*, "Improved Characterization of the Astrophysical Muon–neutrino Flux with 9.5 Years of IceCube Data," *Astrophys. J.* **928** (2022) no.1, 50, doi:10.3847/1538-4357/ac4d29.

[2] K. M. Górski, *et al.*, "HEALPix - A Framework for high resolution discretization, and fast analysis of data distributed on the sphere," *Astrophys. J.* **622** (2005), 759-771, doi:10.1086/427976

[3] S. Alves Garre, *Search for the Origin of Cosmic Rays with the ANTARES Neutrino Telescope*, PhD Thesis, Universitat de València, 2025. https://roderic.uv.es/items/48842bf9-3c16-4398-af38-e40092037fd4

[4] S. P. Wakely and D. Horan, "TeVCat: An online catalog for Very High Energy Gamma-Ray Astronomy," in *Proceedings of the 30th International Cosmic Ray Conference (ICRC)*, vol. 3, pp. 1341–1344, 2008. Available at http://www.tevcat.uchicago.edu.

[5] IceCube Collaboration,"Neutrino emission from the direction of the blazar TXS 0506+056 prior to the IceCube-170922A alert," Science **361** (2018) no.6398, 147-151 doi:10.1126/science.aat2890

[6] G. Illuminati *et al.*, "Searches for Point-like Sources of Cosmic Neutrinos with 15 Years of ANTARES Data," *PoS(ICRC2023)*, 1128 (2023). https://pos.sissa.it/444/1128

[7] D. Dornic for the KM3NeT Collaboration, "The KM3NeT neutrino telescope: status and recent results", these proceedings.

PROCEEDINGS OF SCIENCE

Full Authors List: The ANTARES Collaboration

A. Albert[a,b], S. Alves[c], M. André[d], M. Ardid[e], S. Ardid[e], J.-J. Aubert[f], J. Aublin[g], B. Baret[g], S. Basa[h], Y. Becherini[g], B. Belhorma[i], F. Benfenati[j,k], V. Bertin[f], S. Biagi[l], J. Boumaaza[m], M. Bouta[n], M.C. Bouwhuis[o], H. Brânzaş[p], R. Bruijn[o,q], J. Brunner[f], J. Busto[f], B. Caiffi[r], D. Calvo[c], S. Campion[s,t], A. Capone[s,t], F. Carenini[j,k], J. Carr[f], V. Carretero[c], T. Cartraud[g], S. Celli[s,t], L. Cerisy[f], M. Chabab[u], R. Cherkaoui El Moursli[m], T. Chiarusi[j], M. Circella[v], J.A.B. Coelho[g], A. Coleiro[g], R. Coniglione[l], P. Coyle[f], A. Creusot[g], A. F. Díaz[w], B. De Martino[f], C. Distefano[l], I. Di Palma[s,t], C. Donzaud[g,x], D. Dornic[f], D. Drouhin[a,b], T. Eberl[y], A. Eddymaoui[m], T. van Eeden[o], D. van Eijk[o], S. El Hedri[g], N. El Khayati[m], A. Enzenhöfer[f], P. Fermani[s,t], G. Ferrara[l], F. Filippini[j,k], L. Fusco[z], S. Gagliardini[s,t], J. García-Méndez[e], C. Gatius Oliver[o], P. Gay[aa,g], N. Geißelbrecht[y], H. Glotin[ab], R. Gozzini[c], R. Gracia Ruiz[y], K. Graf[y], C. Guidi[r,ac], L. Haegel[g], H. van Haren[ad], A.J. Heijboer[o], Y. Hello[ae], L. Hennig[y], J.J. Hernández-Rey[c], J. Hößl[y], F. Huang[f], G. Illuminati[j,k], B. Jisse-Jung[o], M. de Jong[o,af], P. de Jong[o,q], M. Kadler[ag], O. Kalekin[y], U. Katz[y], A. Kouchner[g], I. Kreykenbohm[ah], V. Kulikovskiy[r], R. Lahmann[y], M. Lamoureux[g], A. Lazo[c], D. Lefèvre[ai], E. Leonora[aj], G. Levi[j,k], S. Le Stum[f], S. Loucatos[ak,g], J. Manczak[c], M. Marcelin[h], M. Marconi[r,ac], A. Margiotta[j,k], A. Marinelli[al,am], J.A. Martínez-Mora[e], P. Migliozzi[al], A. Moussa[n], R. Muller[o], S. Navas[an], E. Nezri[h], B. Ó Fearraigh[o], E. Oukacha[g], A.M. Păun[p], G.E. Păvălaş[p], S. Peña-Martínez[g], M. Perrin-Terrin[f], P. Piattelli[l], C. Poirè[z], V. Popa[p], T. Pradier[a], N. Randazzo[aj], D. Real[c], G. Riccobene[l], A. Romanov[r,ac], A. Sánchez Losa[c], A. Saina[c], F. Salesa Greus[c], D. F. E. Samtleben[o,af], M. Sanguineti[r,ac], P. Sapienza[l], F. Schüssler[ak], J. Seneca[o], M. Spurio[j,k], Th. Stolarczyk[ak], M. Taiuti[r,ac], Y. Tayalati[m], B. Vallage[ak,g], G. Vannoye[f], V. Van Elewyck[g,ao], S. Viola[l], D. Vivolo[ap,al], J. Wilms[ah], S. Zavatarelli[r], A. Zegarelli[s,t], J.D. Zornoza[c], J. Zúñiga[c].

[a] Université de Strasbourg, CNRS, IPHC UMR 7178, F-67000 Strasbourg, France
[b] Université de Haute Alsace, F-68100 Mulhouse, France
[c] IFIC - Instituto de Física Corpuscular (CSIC - Universitat de València) c/ Catedrático José Beltrán, 2 E-46980 Paterna, Valencia, Spain
[d] Technical University of Catalonia, Laboratory of Applied Bioacoustics, Rambla Exposició, 08800 Vilanova i la Geltrú, Barcelona, Spain
[e] Institut d'Investigació per a la Gestió Integrada de les Zones Costaneres (IGIC) - Universitat Politècnica de València. C/ Paranimf 1, 46730 Gandia, Spain
[f] Aix Marseille Univ, CNRS/IN2P3, CPPM, Marseille, France
[g] Université Paris Cité, CNRS, Astroparticule et Cosmologie, F-75013 Paris, France
[h] Aix Marseille Univ, CNRS, CNES, LAM, Marseille, France
[i] National Center for Energy Sciences and Nuclear Techniques, B.P.1382, R. P.10001 Rabat, Morocco
[j] INFN - Sezione di Bologna, Viale Berti-Pichat 6/2, 40127 Bologna, Italy
[k] Dipartimento di Fisica e Astronomia dell'Università di Bologna, Viale Berti-Pichat 6/2, 40127, Bologna, Italy
[l] INFN - Laboratori Nazionali del Sud (LNS), Via S. Sofia 62, 95123 Catania, Italy
[m] University Mohammed V in Rabat, Faculty of Sciences, 4 av. Ibn Battouta, B.P. 1014, R.P. 10000 Rabat, Morocco
[n] University Mohammed I, Laboratory of Physics of Matter and Radiations, B.P.717, Oujda 6000, Morocco
[o] Nikhef, Science Park, Amsterdam, The Netherlands
[p] Institute of Space Science - INFLPR subsidiary, 409 Atomistilor Street, Măgurele, Ilfov, 077125 Romania
[q] Universiteit van Amsterdam, Instituut voor Hoge-Energie Fysica, Science Park 105, 1098 XG Amsterdam, The Netherlands
[r] INFN - Sezione di Genova, Via Dodecaneso 33, 16146 Genova, Italy
[s] INFN - Sezione di Roma, P.le Aldo Moro 2, 00185 Roma, Italy
[t] Dipartimento di Fisica dell'Università La Sapienza, P.le Aldo Moro 2, 00185 Roma, Italy
[u] LPHEA, Faculty of Science - Semlali, Cadi Ayyad University, P.O.B. 2390, Marrakech, Morocco.
[v] INFN - Sezione di Bari, Via E. Orabona 4, 70126 Bari, Italy
[w] Department of Computer Architecture and Technology/CITIC, University of Granada, 18071 Granada, Spain
[x] Université Paris-Sud, 91405 Orsay Cedex, France
[y] Friedrich-Alexander-Universität Erlangen-Nürnberg, Erlangen Centre for Astroparticle Physics, Erwin-Rommel-Str. 1, 91058 Erlangen, Germany
[z] Università di Salerno e INFN Gruppo Collegato di Salerno, Dipartimento di Fisica, Via Giovanni Paolo II 132, Fisciano, 84084 Italy
[aa] Laboratoire de Physique Corpusculaire, Clermont Université, Université Blaise Pascal, CNRS/IN2P3, BP 10448, F-63000 Clermont-Ferrand, France
[ab] LIS, UMR Université de Toulon, Aix Marseille Université, CNRS, 83041 Toulon, France
[ac] Dipartimento di Fisica dell'Università, Via Dodecaneso 33, 16146 Genova, Italy
[ad] Royal Netherlands Institute for Sea Research (NIOZ), Landsdiep 4, 1797 SZ 't Horntje (Texel), the Netherlands
[ae] Géoazur, UCA, CNRS, IRD, Observatoire de la Côte d'Azur, Sophia Antipolis, France
[af] Huygens-Kamerlingh Onnes Laboratorium, Universiteit Leiden, The Netherlands
[ag] Institut für Theoretische Physik und Astrophysik, Universität Würzburg, Emil-Fischer Str. 31, 97074 Würzburg, Germany
[ah] Dr. Remeis-Sternwarte and ECAP, Friedrich-Alexander-Universität Erlangen-Nürnberg, Sternwartstr. 7, 96049 Bamberg, Germany
[ai] Mediterranean Institute of Oceanography (MIO), Aix-Marseille University, 13288, Marseille, Cedex 9, France; Université du Sud Toulon-Var, CNRS-INSU/IRD UM 110, 83957, La Garde Cedex, France
[aj] INFN - Sezione di Catania, Via S. Sofia 64, 95123 Catania, Italy
[ak] IRFU, CEA, Université Paris-Saclay, F-91191 Gif-sur-Yvette, France
[al] INFN - Sezione di Napoli, Via Cintia 80126 Napoli, Italy

PoS(ICRC2025)1191

[am] Dipartimento di Fisica dell'Università Federico II di Napoli, Via Cintia 80126, Napoli, Italy
[an] Dpto. de Física Teórica y del Cosmos & C.A.F.P.E., University of Granada, 18071 Granada, Spain
[ao] Institut Universitaire de France, 75005 Paris, France
[ap] Dipartimento di Matematica e Fisica dell'Università della Campania L. Vanvitelli, Via A. Lincoln, 81100, Caserta, Italy

Acknowledgements

The authors acknowledge the financial support of the funding agencies: Centre National de la Recherche Scientifique (CNRS), Commissariat à l'énergie atomique et aux énergies alternatives (CEA), Commission Européenne (FEDER fund and Marie Curie Program), LabEx UnivEarthS (ANR-10-LABX-0023 and ANR-18-IDEX-0001), Région Alsace (contrat CPER), Région Provence-Alpes-Côte d'Azur, Département du Var and Ville de La Seyne-sur-Mer, France; Bundesministerium für Bildung und Forschung (BMBF), Germany; Istituto Nazionale di Fisica Nucleare (INFN), Italy; Nederlandse organisatie voor Wetenschappelijk Onderzoek (NWO), the Netherlands; Ministry of Education and Scientific Research, Romania; MCIN for PID2021-124591NB-C41, -C42, -C43 and PDC2023-145913-I00 funded by MCIN/AEI/10.13039/501100011033 and by "ERDF A way of making Europe", for ASFAE/2022/014 and ASFAE/2022 /023 with funding from the EU NextGenerationEU (PRTR-C17.I01) and Generalitat Valenciana, for Grant AST22_6.2 with funding from Consejería de Universidad, Investigación e Innovación and Gobierno de España and European Union - NextGenerationEU, for CSIC-INFRA23013 and for CNS2023-144099, Generalitat Valenciana for CIDEGENT/2020/049, CIDEGENT/2021/23, CIDEIG/2023/20, ESGENT2024/24, CIPROM/2023/51, GRISOLIAP/2021/192 and INNVA1/2024/110 (IVACE+i), Spain; Ministry of Higher Education, Scientific Research and Innovation, Morocco, and the Arab Fund for Economic and Social Development, Kuwait. We also acknowledge the technical support of Ifremer, AIM and Foselev Marine for the sea operation and the CC-IN2P3 for the computing facilities.